

# Parameterization for $q_T$ -spectrum of inclusive $Z$ -boson hadroproduction

M.V. Bondarenko,\* S.T. Lukyanenko, and P.V. Sorokin

*NSC Kharkov Institute of Physics and Technology, 1 Academic St., 61108 Kharkov, Ukraine*

(Dated: November 11, 2018)

We propose a simple parameterization for  $q_T$ -spectrum of inclusive  $Z$ -boson production, and test it against world collider data at different energies. The fit gives good agreement with the data, and indicates the existence of two distinguishable breaks in the  $q_T$ -spectrum. Energy dependences of the fitted parameters are discussed.

PACS numbers: 13.85.Qk, 12.38.Bx, 12.15.Ji

Momentum distributions of heavy bosons ( $W^\pm$ ,  $Z$ , or highly virtual photons) inclusively produced in hadron-hadron collisions [1, 2] are widely used for studies of the underlying parton interaction subprocesses, as well as parton distribution functions (pdfs) [3, 4]. At high collision energy  $\sqrt{s}$ , the dependences on the boson transverse momentum  $q_T$  (with respect to the hadron collision axis) and on the boson rapidity  $Y$  correlate only weakly, so it makes good sense first to study single-differential normalized cross-sections  $\frac{1}{\sigma} \frac{d\sigma}{dq_T}$  and  $\frac{1}{\sigma} \frac{d\sigma}{dY}$  independently. In this Letter, we will discuss some trends emerging in the behavior of the  $q_T$ -spectrum at highest accessible  $\sqrt{s}$ .

As has long been known,  $q_T$ -spectra of heavy boson production contain several distinct kinematic regions. In the hard region  $q_T \gtrsim M_V$ , with  $M_V$  the boson (or dilepton) mass, perturbative calculations are expected to be reliable. In the Sudakov region, where  $q_T \ll M_V$ , partonic differential cross-sections are enhanced, favoring resummation to all orders of perturbation theory [5, 6]. That is equivalent to account of parton cascading effects. Finally, there is a soft and genuinely non-perturbative region  $q_T \sim 1$  GeV, where hadronic degrees of freedom in cascading become essential.

At present, the theoretical framework for treatment of the boson  $q_T$ -spectrum simultaneously in all regions reached high degree of sophistication [7–10], involving a host of adjustable parameters entering the pdfs, the factorization and renormalization schemes, and infrared regulators. On the other hand, the experimental shape of the boson  $q_T$ -spectrum does not exhibit many features, so, it can tightly constrain only a few parameters or their combinations.

Our observation made when working with high-statistics data (specified below) is that in region  $q_T \ll M_V$ , the spectrum basically follows a power-law pattern, whereas at asymptotic  $q_T \gg M_V$ , it changes to a power law with a greater spectral index. Even though there are no firm theoretical reasons for a strictly power-like behavior anywhere [25], it may serve as a fair approximation in an available limited range of  $q_T$ . In total, two power laws contain 2 spectral indices and 2 scales (or normalizations), hence the minimal number of param-

eters required to describe the complete boson production  $q_T$ -spectrum equals 4.

The transition between the intervals of power-law behavior is smooth, yet it may be smeared out by poor statistics data. But nowadays, high-statistics data are delivered by the Tevatron and the LHC, which may provide a sharper picture of this transition.

In the present Letter, we propose a simple 4-parameter model for the differential cross-section, and test it against the best data presently available at different energies. Those data include the Tevatron CDF measurement of  $p\bar{p} \rightarrow e^+e^-X$  production at  $\sqrt{s} = 1.98$  TeV, with 2.1 fb $^{-1}$  of integrated luminosity [12], and the LHC measurement at  $\sqrt{s} = 7$  TeV in channels  $pp \rightarrow \mu^+\mu^-X, e^+e^-X$ , with 36 pb $^{-1}$  of integrated luminosity [13, 14]. To be more certain about the trends, we add results of the  $S\bar{p}pS$  UA2 experiment at  $\sqrt{s} = 0.63$  TeV [15], which has ample statistics in channel  $p\bar{p} \rightarrow e\nu X$  (at the  $W$  resonance), although restricted to the region of low  $q_T$  only. The  $q_T$ -spectrum shape for  $W$ -boson production is expected to be about the same as for  $Z$ , inasmuch as  $M_W \approx M_Z$ , and furthermore, since in the covered region  $q_T \ll M_W$ , the  $q_T$ -spectrum should have little sensitivity to the value of  $M_W$  (as if  $M_W$  was sent to infinity at  $q_T$  fixed). All the above mentioned measurements are rapidity-inclusive and select events in a broad vicinity of the electroweak boson mass resonance.

The ansatz we adopt for the  $q_T$ -spectrum reads

$$\frac{1}{\sigma} \frac{d\sigma}{dq_T^2} = \frac{1}{N} \frac{dN}{dq_T} = \frac{A(a, \kappa, M, \nu)}{(1 + q_T^2/a^2)^{1+\kappa} (1 + q_T^2/M^2)^{1+\nu}} q_T, \quad (1)$$

where  $a, \kappa, M, \nu$  are the adjustable parameters. Factor  $q_T$  in (1) stems from the correspondence  $\frac{d\sigma}{dq_T} = 2q_T \frac{d\sigma}{dq_T^2}$ , while  $\frac{d\sigma}{dq_T^2} = \pi \frac{d\sigma}{dq_x dq_y}$  in our axially symmetric geometry must be an entire function of  $q_T^2 = q_x^2 + q_y^2$ . Parameter  $M$  is not to be confused with the electroweak boson mass, although we expect it to be of the same order. Numerator  $A(a, \kappa, M, \nu)$  in (1) is fixed by the normalization

\*Electronic address: bon@kipt.kharkov.ua

condition  $\int_0^\infty dq_T \frac{1}{\sigma} \frac{d\sigma}{dq_T} \equiv 1$ , giving

$$\frac{2}{A} = \frac{a^2}{1 + \kappa + \nu} F\left(1 + \nu, 1; 2 + \kappa + \nu; 1 - \frac{a^2}{M^2}\right) \quad (2a)$$

$$\begin{aligned} &\equiv \frac{a^2}{\kappa} F\left(1 + \nu, 1; 1 - \kappa; \frac{a^2}{M^2}\right) \\ &+ \frac{a^{2(1+\kappa)} M^{2(1+\nu)}}{(M^2 - a^2)^{1+\kappa+\nu}} B(1 + \kappa + \nu, -\kappa), \end{aligned} \quad (2b)$$

where  $B$  is the Euler beta function, and  $F$  the hypergeometric function. If  $a \ll M$ , Eq. (2b) simplifies to

$$\frac{2}{Aa^2} = \frac{1}{\kappa} \left[ 1 - \left(\frac{a}{M}\right)^{2\kappa} \frac{\Gamma(1 + \kappa + \nu)\Gamma(1 - \kappa)}{\Gamma(1 + \nu)} \right] + \mathcal{O}\left(\frac{a^2}{M^2}\right), \quad (3)$$

where the second term in brackets, albeit formally small if ratio  $a/M \ll 1$ , at practice can be  $\sim 0.3$ , and thus non-negligible. Also note that in the formal limit  $\kappa \rightarrow 0$ , the second term in brackets in (3) behaves as  $1 + \mathcal{O}(\kappa)$ , thus canceling the singularity due to overall factor  $\kappa^{-1}$ .

Algebraic structure (1) is intended to arrange a simple interpolation between limiting cases where certain expectations about the spectrum behavior can be stated. Those limiting cases are described below.

At  $q_T \ll M$ , Eq. (1) simplifies to

$$\frac{1}{\sigma} \frac{d\sigma}{dq_T} \simeq \frac{A}{(1 + q_T^2/a^2)^{1+\kappa}} q_T. \quad (4a)$$

Parameter  $a$  regularizes the differential cross-section in the small- $q_T$  region, where there is no reliable *ab initio* theoretical treatment, anyway. Parameterization of type (4a) had been phenomenologically successful for description of  $q_T$ -spectra of light hadrons produced in high-energy collisions (see, e.g., [16]), and of low-mass dilepton pairs at moderate energies [17], with parameter  $\kappa \sim 4-5$ . In our problem, though, we do not expect index  $\kappa$  to be that high, because  $Z$ -boson is a structureless particle (in contrast to secondary hadrons), and because at large collider energies, the participating partons have momentum fractions  $x$  far from the valence region where gluon and antiquark pdfs receive additional suppression [4]. Specific forms for low- $q_T$  parameterization may vary: in particular, a thermodynamically-inspired Tsallis [18, 19] form has been popular:

$$\frac{1}{\sigma} \frac{d\sigma}{dq_T} \simeq \frac{A}{(1 + q_T/q_0)^n} q_T, \quad (4b)$$

but it has a formal deficiency of being non-analytic in  $q_T$ -plane at  $q_x = q_y = 0$ . [26] We refrain from thermodynamic analogies for our process, assuming it to be governed by particle cascading in free space.

In the Sudakov region  $a \ll q_T \ll M$ , both Eq. (4a) and (4b) reduce to a power law

$$\frac{1}{\sigma} \frac{d\sigma}{dq_T} \simeq \frac{Aa^{2(1+\kappa)}}{q_T^{1+\kappa}}. \quad (5)$$

When the boson production is calculated by pQCD [see subprocesses (10) below], the leading logarithmic asymptotics for subprocess (10a) would correspond to behavior  $\frac{d\sigma_{q\bar{q}}}{dq_T} \propto \frac{\alpha_s}{q_T}$ , while that for subprocess (10b), to  $\frac{d\sigma_{q\bar{q}}}{dq_T} \propto \frac{\alpha_s}{q_T} \log \frac{M_V}{q_T}$  [2, 20]. The latter behavior can mimic power law (5) with small and positive  $\kappa$ . On the other hand, resummation of large logarithms to all orders in  $\alpha_s$  can manifest itself as small [ $\sim \alpha_s(M_V)$ ] but negative contribution to  $\kappa$ . We will not contemplate theoretical estimates of  $\kappa$  here, leaving it for experiment. In what concerns consequences for parameter  $a$ , obviously, with the increase of  $\sqrt{s}$ , momentum fractions  $x$  of participating partons diminish, and the number of parton branchings increases. By analogy with DIS, that should lead to transverse momentum broadening [21]. Hence,  $a$  is expected to increase with  $\sqrt{s}$ .

On a log-log plot, any power law, in particular, intermediate asymptotics (5), and the ultra-low- $q_T$  asymptotics

$$\frac{1}{\sigma} \frac{d\sigma}{dq_T} \simeq Aq_T \quad (\text{at } q_T \ll a), \quad (6)$$

is represented by a straight line. Function (4a) then describes a transition between straight line behaviors of (5) and (6). It features a break at  $q_T \sim a$ , which will be called the 1st break – see Fig. 1a.

At  $q_T \gg M$ , Eq. (1) reduces to another power law:

$$\frac{1}{\sigma} \frac{d\sigma}{dq_T} \simeq \frac{Aa^{2(1+\kappa)} M^{2(1+\nu)}}{q_T^{3+2(\kappa+\nu)}}. \quad (7)$$

Since thereat the boson mass can be neglected, this case must be close to production of real photons. The transverse energy spectrum of the latter process is known to fall off as  $\frac{1}{\sigma} \frac{d\sigma^\gamma}{dq_T} \propto q_T^{-5.4}$  for the Tevatron [22], and  $\propto q_T^{-4.5}$  for the LHC [23], wherefrom we expect

$$\kappa + \nu \approx 1.2 \quad (\text{Tevatron}), \quad (8a)$$

$$\kappa + \nu \approx 0.75 \quad (\text{LHC}). \quad (8b)$$

Note that physically, the behavior of the massive boson production differential cross-section at high  $q_T$  is sensitive to behavior of the hadron pdfs, thus, determination of  $\kappa + \nu$  at high  $\sqrt{s}$  allows constraining small- $x$  pdf slopes at  $Q^2 \gtrsim M_V^2$ .

The transition between power-law regions (5) and (7) is described by formula

$$\frac{1}{\sigma} \frac{d\sigma}{dq_T} \simeq \frac{Aa^{2(1+\kappa)}}{q_T^{1+2\kappa} (1 + q_T^2/M^2)^{1+\nu}}, \quad (9)$$

obtained from (1) by neglecting the unity in the first factor in the denominator. Similarly to (4a), it features a break on a log-log plot at  $q_T \sim M$ , which will be called the 2nd break (see Fig. 1a). The physical motivation for structure (9) is that in the perturbative region, the boson

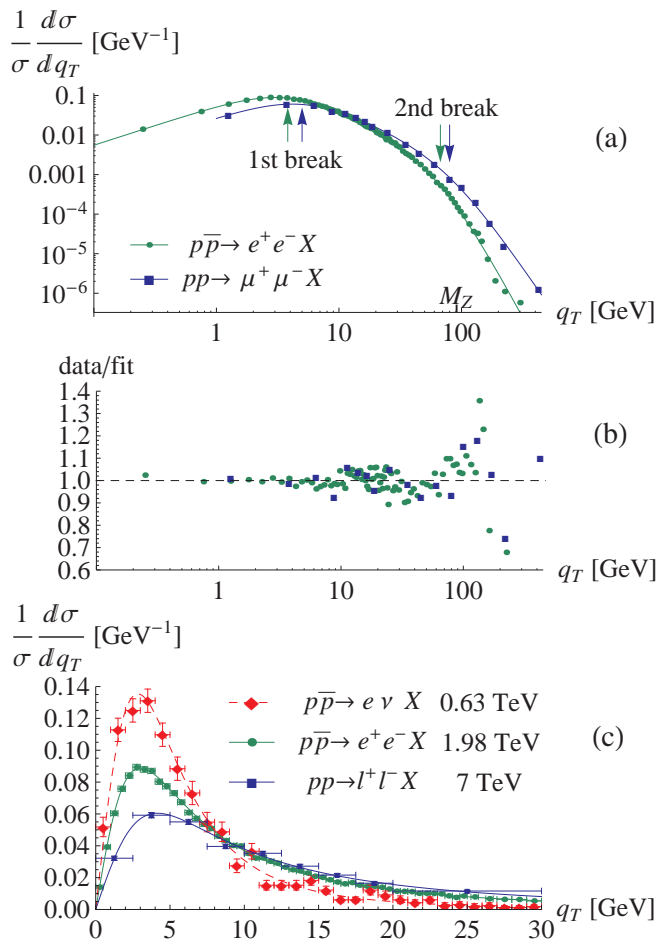


FIG. 1: Comparison of fits to electroweak boson  $q_T$ -distributions for different collision energies. (a) The full experimental  $q_T$  range. Green points and the curve, the Tevatron [12]; blue points and the curve, the LHC [13]. The arrows show break positions (values of  $a$  and  $M$ ) for each curve. (b) Data to fit ratio for same experiments. (c) The small- $q_T$  region. Green and blue points and curves, same as in (a,b). Red points and the dashed curve stand for  $W$ -boson production at the  $S\bar{p}pS$  [15].

is expected to be produced chiefly through  $2 \rightarrow 2$  parton reactions

$$\text{quark(antiquark)} + \text{gluon} \rightarrow \text{quark(antiquark)} + \text{boson}, \quad (10a)$$

$$\text{quark} + \text{antiquark} \rightarrow \text{gluon} + \text{boson}, \quad (10b)$$

in which the boson's transverse momentum is balanced by that of a final parton subsequently transforming into a hadronic jet. Calculations of those reactions indicate that they indeed form up a break in the boson's  $q_T$ -spectrum, although block 1 +  $q_T^2/M_V^2$  enters there in a more complicated fashion than in (1). Such a break has so far not been established experimentally, so our goal will be to examine whether it manifests itself in the new data.

Our approach to handling the data is as follows. Experimental  $q_T$ -spectra of electroweak boson hadropro-

TABLE I: The fitted parameter values for experiments [15], [12, 13]. The indicated errors are standard deviations.

$\sqrt{s}$ , TeV	$a$ , GeV	$\kappa$	$M$ , GeV	$\nu$	$\kappa + \nu$
0.63	$5.0 \pm 0.6$	$1.1 \pm 0.1$	–	–	–
1.98	$3.8 \pm 0.3$	$0.29 \pm 0.04$	$67 \pm 5$	$1.1 \pm 0.1$	$1.4 \pm 0.1$
7	$5.1 \pm 0.6$	$0.23 \pm 0.08$	$80 \pm 13$	$0.54 \pm 0.09$	$0.8 \pm 0.1$

duction [12–15] are published in form of a cross-section per bin of  $q_T$ . We ascribe the locations of experimental points to the bin centres, neglecting the associated biases. Thereupon, we fit[27] our model (1) to the data points for experiments [12, 13], and the reduced model (4a) to the low- $q_T$  data of experiment [15]. The overall normalization coefficient  $A$  is chosen to obey Eq. (2a), although nothing essentially changes if  $A$  is treated as an independent adjustable parameter.

The fit results are summarized in Figs. 1 and Table I. Since the parameterization follows the data closely, and all the parameters are constrained tightly, our model may be regarded as phenomenologically reasonable. The existence of a two-break structure of the  $q_T$ -spectrum is thus likely, although there is little room for intermediate asymptotics (5). Fig. 1b shows the data to fit ratio as a function of  $q_T$ . For the LHC experiment, the deviations seem to be random, whereas for the Tevatron experiment, there are sign-alternating systematic deviations on the level of 5–10%, though they are also commensurable with statistical fluctuations. Naturally, our simple model can not capture all the physical subtleties; rather, it is surprising that its systematic deviations are so small.

The obtained parameter values and their differences between the Tevatron and the LHC conditions deserve some physical discussion. First of all, since  $a$  and  $M$  prove to differ by more than an order of magnitude, the hard and soft scales in our problem are sufficiently well separated. Secondly, it confirms that  $M \sim M_Z$ , although the actual value of  $M$  appears to be somewhat smaller than  $M_Z$ .

Next, values of the total spectral index  $\kappa + \nu$  in Table I agree with the differential spectral index for direct photon production [cf. Eqs. (8)]. For the Tevatron,  $\kappa + \nu \approx 1.4$  is appreciably greater than the corresponding value 0.8 for the LHC. That must be attributed to the fact that at the Tevatron energy, the small- $x$  regime at  $q_T > 100$  GeV is not reached yet (in contrast to the small- $q_T$  domain), and there is extra suppression of antiquark and gluon distributions in the valence region.

Index  $\kappa$  alone both for the Tevatron and the LHC is small and positive. Still, it is not quite clear whether it remains  $\sqrt{s}$ -dependent at  $\sqrt{s} \rightarrow \infty$ . For the  $S\bar{p}pS$  experiment, parameter  $\kappa \approx 1.1$  is rather large, merely because at this energy, the partons are characterized by sizable  $x \sim M_W/\sqrt{s} = 0.13$ , where antiquark and gluon pdfs experience valence domain suppressions. But for the Tevatron and the LHC, the values of  $\kappa$  are commen-

surable, indicating that at the Tevatron energy, small- $x$  approximation holds fairly well for moderate  $q_T$  already. Hence, the proportion between contributions from reactions (10a) and (10b) at the Tevatron and the LHC may be about the same, though not exactly.

Finally, at small  $q_T$ , the normalized spectrum is essentially characterized by parameter  $a$  alone (given that  $\kappa$  is small enough). In the past [1], it had been common to characterize the spectrum width by the mean transverse momentum  $\langle q_T \rangle = \int_0^\infty dq_T q_T \frac{1}{\sigma} \frac{d\sigma}{dq_T}$ . However, low- $q_T$  approximation (4a) cannot be used for that purpose, as long as for  $\kappa < \frac{1}{2}$ , the spectrum has a too slowly decreasing ‘tail’, wherewith  $\langle q_T \rangle$  diverges. When evaluated by complete formula (1), the mean transverse momentum equals

$$\begin{aligned} \langle q_T \rangle &= \frac{a^3 A}{2} \left\{ B\left(\frac{3}{2}, \kappa - \frac{1}{2}\right) F\left(\frac{3}{2}, 1 + \nu, \frac{3}{2} - \kappa, \frac{a^2}{M^2}\right) \right. \\ &\quad \left. + B\left(\kappa + \nu + \frac{1}{2}, \frac{1}{2} - \kappa\right) \left(\frac{M}{a}\right)^{1-2\kappa} \right. \\ &\quad \left. \times F\left(\kappa + \nu + \frac{1}{2}, 1 + \kappa, \kappa + \frac{1}{2}, \frac{a^2}{M^2}\right) \right\} \\ &\approx a \left\{ B\left(\frac{3}{2}, \kappa - \frac{1}{2}\right) + B\left(\kappa + \nu + \frac{1}{2}, \frac{1}{2} - \kappa\right) \left(\frac{M}{a}\right)^{1-2\kappa} \right\}. \end{aligned} \quad (11)$$

If  $\kappa$  was greater than  $1/2$  (as for the  $S\bar{p}pS$  conditions), the second term in (11) would be subdominant, owing to  $(M/a)^{1-2\kappa}$  factor. However, for the Tevatron and LHC conditions, where  $\kappa < 1/2$ , on the contrary, the second term in (11) dominates and makes  $\langle q_T \rangle$  a few times greater than  $a$ . Therefore, at multi-TeV energies, parameter  $a$  is arguably better suited for characterization of the spectrum width than  $\langle q_T \rangle$ . The maximum of spectrum  $\frac{1}{\sigma} \frac{d\sigma}{dq_T}$  is achieved at  $q_T \approx \frac{a}{\sqrt{1+2\kappa}} \sim a$ , and its height basically scales as  $\sim a^{-1}$ , because it equals  $\sim Aq_T$  with  $A \sim a^{-2}$  [see Eq. (3)].

The formidable magnitude of  $a$  compared to typical hadron mass scale is not unusual for semi-inclusive high-energy reactions [2, 7–10]. It suggests that  $a$  may involve a weak dependence on hard scales  $M_V$ ,  $\sqrt{s}$ . In this regard, interesting is the noticeable difference between the fitted values of  $a$  for the Tevatron and the LHC. That hints that  $a$  may slowly increase with  $\sqrt{s}$  starting from the Tevatron energy (cf. [21]). (Therewith,  $\langle q_T \rangle$  given by

Eq. (11) will grow, as well.) This is in line with the general trend of the electroweak boson  $q_T$ -spectrum broadening continuing since the  $S\bar{p}pS$  (see Fig. 1c). Although the value of  $a$  for the  $S\bar{p}pS$  is actually greater than for higher-energy experiments, that may be merely an artifact of much greater  $\kappa$ , which, as we argued before, originates from effects of valence-region suppression at moderate  $S\bar{p}pS$  energy.

We end up with a remark that factor

$$(1 + q_T^2/a^2)^{-1-\kappa} \quad (12)$$

in (4a) with  $\kappa \sim 0.25$  is reminiscent of the Cauchy distribution in 2 dimensions [24]:

$$(1 + q_T^2/a^2)^{-3/2}, \quad (13)$$

corresponding to  $\kappa = 1/2$ . The key property of the latter distribution is its Lévy-stability under  $q_T$ -convolutions. Such a stability may be physically relevant inasmuch as during cascading in the boson production process, the particles undergo successive transverse momentum redistributions. Stable distributions exist at  $\kappa \neq 1/2$  as well, though they do not assume algebraic form. But rough closeness of  $1 + \kappa$  to  $3/2$  may explain the phenomenological success of algebraic form (12). Also note that since hadron branching effects obscure the dependence of  $\frac{d\sigma}{dq_T}$  on intrinsic parton transverse momentum distributions in initial hadrons, 2-scale factorization of type (1) may be more practical than factoring out the transverse momentum-dependent pdfs and the resummed hard scattering factor (cf. [5, 8]).

Summarizing, the second break in the  $q_T$ -spectrum of  $Z$ -boson hadroproduction begins to manifest itself at TeV energies, and its location is close to the  $Z$ -boson mass. Energy-dependences of parameters of our parameterization (1) are interesting. In particular, they indicate gradual spectrum broadening and increase of  $a$  with  $\sqrt{s}$ , as well as slowdown of  $\sqrt{s}$ -dependences of spectral indices  $\kappa$  and  $\nu$ . The practical value of extraction of those indices is that  $\kappa$  should be sensitive to parton kinetics in the Regge region, and could be valuable for resummation studies, while the total spectral index  $\kappa + \nu$  must be closely related to the index of power-law rise of parton pdfs at small  $x$ .

- 
- [1] R. Stroynowski, Phys. Rep. **71**, 1 (1981);  
G. Altarelli, Phys. Rep. **81**, 1 (1982).  
[2] R.K. Ellis, W.J. Stirling, B.R. Webber. *QCD and Collider Physics* (Cambridge, Univ. Press, 2003).  
[3] M. Dittmar *et al.* arXiv:0511119 [hep-ph].  
[4] H.-L. Lai *et al.* Phys. Rev. D **82**, 074024 (2010);  
A.D. Martin *et al.* Eur. Phys. J. **63**, 189 (2009);  
R.D. Ball *et al.* Nucl. Phys. B **838**, 136 (2010).  
[5] Yu.L. Dokshitzer, D.I. Dyakonov, and S.I. Troyan, Phys. Rep. **68**, 269 (1980).  
[6] G. Parisi and R. Petronzio, Nucl. Phys. B **154**, 427 (1979).  
[7] J. Collins, D. Soper, and G. Sterman, Nucl. Phys. B **250**, 199 (1985).  
[8] R.K. Ellis and S. Veseli, Nucl. Phys. B **511**, 649 (1997).  
[9] C. Balazs and C.-P. Yuan, Phys. Rev. D **56**, 5558 (1997).  
[10] A. Buckley *et al.* Phys. Rep. **504**, 145 (2011).  
[11] A. De Rujula *et al.* Phys. Rev. D **10**, 1649 (1974);

- R.D. Ball and S. Forte, Phys. Lett. B **335**, 77 (1994).
- [12] T. Aaltonen *et al.* Phys. Rev. D **86**, 052010 (2012).
- [13] S. Chatrchyan *et al.* Phys. Rev. D **85**, 032002 (2012).
- [14] G. Aad *et al.* Phys. Lett. B **705**, 415 (2011).
- [15] J. Alitti *et al.* Zeit. Phys. C **47**, 523 (1990).
- [16] C.Y. Wong and G. Wilk, Phys. Rev. D **87**, 114007 (2013).
- [17] J.K. Yoh *et al.* Phys. Rev. Lett. **41**, 684 (1978);  
A.S. Ito *et al.* Phys. Rev. D **23**, 604 (1981).
- [18] C. Tsallis, J. Stat. Phys. **52**, 479 (1988);  
S. Abe, Y. Okamoto. *Nonextensive Statistical Mechanics and Its Applications* (Springer-Verlag, 2001).
- [19] R. Hagedorn, Riv. Nuov. Cim. **6**, 1 (1984).
- [20] K. Kajantie and R. Raitio, Nucl. Phys. B **139**, 72 (1978).
- [21] S. Berge *et al.* Phys. Rev. D **72**, 033015 (2005).
- [22] T. Aaltonen *et al.* Phys. Rev. D **80**, 111106 (2009).
- [23] S. Chatrchyan *et al.* Phys. Rev. D **84**, 052011 (2011);  
G. Aad *et al.* Phys. Lett. B **706**, 150 (2011).
- [24] V.V. Uchaikin, V.M. Zolotarev. *Chance and Stability. Stable distributions and their applications* (Utrecht, VSP, 1999).
- [25] Strictly speaking, at  $q_T \ll M_V$  one expects an exponentiated double-logarithmic asymptotics of the  $q_T$ -spectrum [6], whereas at  $q_T \gg M_V$ , the  $q_T$ -spectrum is proportional to the underlying pdfs, with their  $x$ 's proportional to  $q_T$ . The pdfs at small  $x$  (if  $\sqrt{s} \gg q_T$ ) may also have exponentiated double-logarithmic asymptotics [3, 11], though can as well admit power-law (Regge) parameterizations [3].
- [26] Owing to this, (4b) gives a somewhat worse fit at small  $q_T$  than (4a) (see [16]).
- [27] To gain sufficient sensitivity of the fit parameters in the large- $q_T$  region, where the spectrum falls off by several orders of magnitude, we are actually fitting the spectrum logarithm.